

RSC Advances



This is an *Accepted Manuscript*, which has been through the Royal Society of Chemistry peer review process and has been accepted for publication.

Accepted Manuscripts are published online shortly after acceptance, before technical editing, formatting and proof reading. Using this free service, authors can make their results available to the community, in citable form, before we publish the edited article. This *Accepted Manuscript* will be replaced by the edited, formatted and paginated article as soon as this is available.

You can find more information about *Accepted Manuscripts* in the [Information for Authors](#).

Please note that technical editing may introduce minor changes to the text and/or graphics, which may alter content. The journal's standard [Terms & Conditions](#) and the [Ethical guidelines](#) still apply. In no event shall the Royal Society of Chemistry be held responsible for any errors or omissions in this *Accepted Manuscript* or any consequences arising from the use of any information it contains.

Cite this: DOI: 10.1039/c0xx00000x

www.rsc.org/xxxxxx

ARTICLE TYPE

Dispersion-controlled PtCu clusters synthesized with citric acid using galvanic displacement with high electrocatalytic activity toward methanol oxidation

Qing Lv,^{a,b} Jinfa Chang,^{a,b} Wei Xing^{*a} and Changpeng Liu^{*c}

Received (in XXX, XXX) Xth XXXXXXXXX 20XX, Accepted Xth XXXXXXXXX 20XX
DOI: 10.1039/b000000x

Dispersion-controlled carbon supported PtCu clusters was firstly synthesized using galvanic displacement of Cu/C, in which citric acid worked as the dispersion agent and its concentration was adjusted to form the as-synthesized clusters. It was found that the well dispersion played a significant role in tuning activity for methanol electrooxidation.

Direct methanol fuel cells (DMFCs) hold great potential as a clean energy source for powering portable electronic devices and vehicles.¹⁻⁵ Currently, Pt-based nanomaterials are the most effective electrocatalysts to facilitate the anodic methanol oxidation reaction,^{1, 6, 7} due to their unique catalytic properties in fuel cells.⁷⁻¹⁵ However, the high cost of the noble metal platinum and low activities of the anode catalysts at room temperature are still one of the important hindlers for the commercialization of DMFCs.^{2, 16-18} To increase the methanol oxidation activity and reduce platinum loading, bimetallic catalysts of platinum alloyed with a less expensive metal and unique morphologies are often used.^{1, 6, 7, 19}

It is generally known that the size, shape, composition and structure of Pt-based catalysts are important parameters which determine the catalytic activity.^{13, 15, 20-24} Galvanic replacement is an effective method that can control the synthesis of Pt-based nanomaterials with special shape and composition.²²⁻²⁴ For example, Pt hollow nanosphere catalyst was developed using galvanic displacement with Co nanoparticles as sacrificial templates, which has a higher surface area and therefore exhibits enhanced electrocatalytic performance.²⁵ Ultrathin PtPdTe and PtTe nanowires were synthesized by using Te nanowires as both sacrificial templates and reducing agents, which induce a higher activity toward the methanol oxidation reaction in comparison with commercial Pt/C.¹⁸ For the galvanic displacement of Cu, the replacement of Cu UPD monolayer by a series of noble metals or their mixtures has been reported for many years, which can only occur on the surface of electrode. In the bulk preparation, because of the ease for Cu to be oxidized, only few authors reported on the galvanic replacement process with Pt. In the recent reports, PtCu/C electrocatalysts were prepared by partial galvanic replacement of Cu/C and exhibited high electrocatalytic activity for methanol oxidation²⁶ and oxygen reduction reaction²². In both reports, PtCu/C was synthesized by a separated two-step

procedure. However, the PtCu nanoparticles were aggregated severely²², which would affect the electrochemical surface area and electron transfer.

Herein, PtCu/C catalysts were successfully prepared by galvanic replacement of Cu/C using a successive two-step procedure. With the protection of Ar during the whole reaction process, this method overcomes the oxidation of Cu issue. The dispersion of PtCu nanoparticles were tuned by adjusting the concentration of citric acid with a series of CuCl₂ : citric acid molar ratio (1 : 0, 2 : 1, 1 : 1, 1 : 2, 1 : 5 denoted as PtCu/C-1, PtCu/C-2, PtCu/C-3, PtCu/C-4 and PtCu/C-5, respectively.) during the replacement process. All the as-synthesized PtCu/C exhibited higher activity for methanol oxidation than commercial Pt/C (Pt/C-C) and home-made Pt/C prepared by traditional method (Pt/C-H) and PtCu/C-3 was evaluated as the most active catalyst. The X-ray photoelectron spectroscopy (XPS) and electrochemical test detected no unstable Cu atoms on the surface of the metal nanoparticles. This property may contribute the as-synthesized PtCu/C catalysts to possessing comparable stability with Pt/C-C and Pt/C-H.

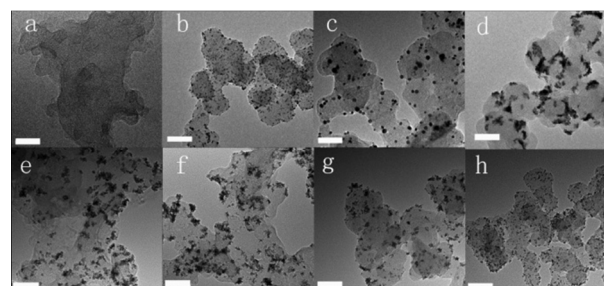


Fig. 1 TEM images of Cu/C (a), Pt/C-C (b), Pt/C-H (c), PtCu/C-1 (d), PtCu/C-2 (e), PtCu/C-3 (f), PtCu/C-4 (g), PtCu/C-5 (h). Scale bars are all 50 nm.

Fig. 1 shows the TEM images of PtCu/C nanocatalysts, Pt/C-H and Pt/C-C, which exhibit remarkable different morphologies. Due to the low diffraction contrast of Cu, the Cu atoms cannot be seen clearly in the TEM image. However, by careful observation and statistics, it can be seen that Cu nanoparticles with the average size of about 1 nm disperses uniformly on the carbon surface (Fig. 1a). The average size of Pt nanoparticles for Pt/C-C and Pt/C-H are 2.45 nm and 5.0 nm, respectively (Fig. 1b and c). By galvanic displacement, PtCu nanoclusters become ribbon –

shape (Fig. 1d). With the addition of citric acid, the shape of PtCu particles looks like fluffy nanoflowers and the size of the nanoflowers become smaller, when the amount of citric acid was increased (Fig. 1e, f and g). For Fig. 1h, the molar ratio of CuCl₂ : citric acid as 1:5, the PtCu nanoclusters become small nanoparticles with uniform size. The shape change of PtCu nanoclusters can be understood easily. In order to decrease the surface energy, the obtained Pt nanoparticles by galvanic displacement like to attach to each other without the addition of citric acid. However, with the addition of citric acid, the nanoparticles are protected by citric acid and PtCu nanoclusters become small nanoflowers. The size of the nanoflowers gets smaller and finally become nanoparticles, when the concentration of citric acid is increased. The metal loading of the catalysts were determined by ICP-MS (Table S1). From the result and the amount of added precursor, we can calculate that almost all the H₂PtCl₆ was reduced by Cu.

The crystalline structures of the catalysts are characterized by X-ray diffraction (XRD) (Fig. S1). Each pattern of the catalysts shows a face-centred cubic phase and the unique series of three diffraction peaks for PtCu/C catalysts have a positive shift, compared with Pt/C-C and Pt/C-H, indicating the alloy formation in all the PtCu/C catalysts^{27,28}. XPS was employed to investigate the electronic property and surface species of the catalyst (Fig. S2). The Pt 4f peaks for the entire PtCu/C shift negatively, compared to that of Pt/C-C and Pt/C-H, which is beneficial to the oxidation of CO. Fig. S2B shows the Cu 2p region of PtCu/C. There is no characteristic peak of Cu for the catalysts, which means no Cu atoms on the surface of PtCu/C catalysts. The absence of Cu on the surface of PtCu/C can also be demonstrated by the cyclic voltammograms (CV) curves in H₂SO₄ which has no oxidation peak of Cu in ca. 0.3 V vs. SCE (Fig. S3).

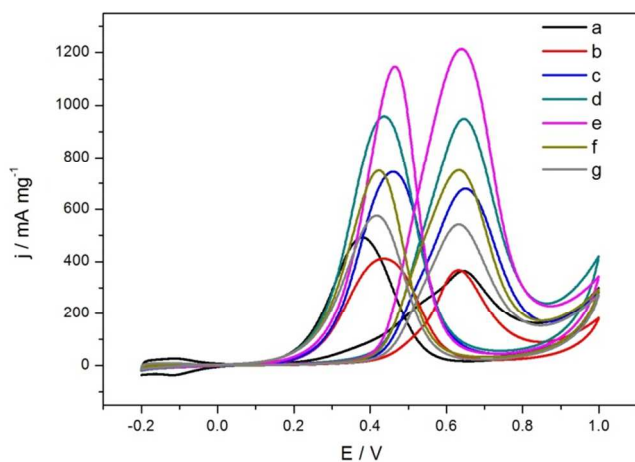


Fig. 2 CV of methanol oxidation on Pt/C-C (a), Pt/C-H (b), PtCu/C-1 (c), PtCu/C-2 (d), PtCu/C-3 (e), PtCu/C-4 (f) and PtCu/C-5 (g) in 0.5 M H₂SO₄ + 1.0 M CH₃OH solution at the scan rate of 50 mV s⁻¹.

Next we tested our as-synthesized PtCu/C catalysts in the electrical catalytic reaction and compared the results with that of the as prepared Pt/C-H and Pt/C-C. Fig. 2 details the CV of the catalysts normalized to the mass of Pt. It can be seen that all the PtCu/C catalysts have higher forward oxidation peak current density than Pt/C-H and Pt/C-C and PtCu/C-3 exhibits the highest peak current density which is ca. 3.3 times than that of Pt/C-H and Pt/C-C. Chronoamperometry (CA) was performed to

investigate the long-term stability of the catalyst for the methanol oxidation reaction (Fig. S4). Given that the “stability” could be defined as the decay rate of the electrode²⁹, the current was normalized to the initial current at 100 s to eliminate the difference in the initial current of the catalysts. The residual ratio for Pt/C-C, Pt/C-H, PtCu/C-1, PtCu/C-2, PtCu/C-3, PtCu/C-4 and PtCu/C-5 are 65.6%, 62.2%, 69.6%, 77.8%, 71.0%, 67.8% and 67.9%, respectively, near to each other. No decrease of stability for PtCu/C catalysts may attribute to the absence of defective unstable Cu atoms on the surface of the nanoclusters.

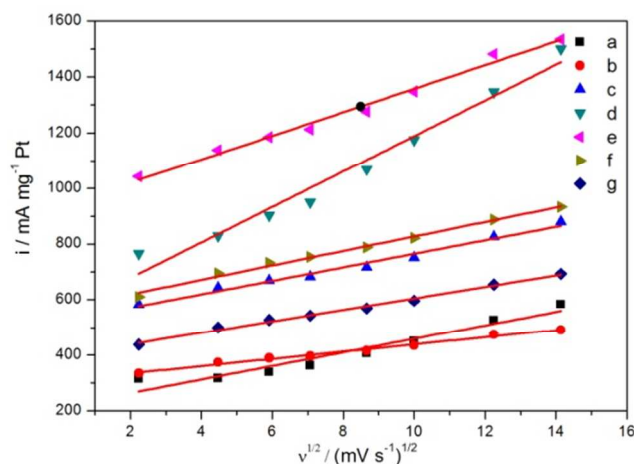


Fig. 3 The linear relationship between peak current density and the square root of the scan rates for Pt/C-C (a), Pt/C-H (b), PtCu/C-1 (c), PtCu/C-2 (d), PtCu/C-3 (e), PtCu/C-4 (f) and PtCu/C-5 (g).

To explore the reasons for the high catalytic activity of PtCu/C, the CVs for the methanol oxidation with different scan rates of 5, 20, 35, 50, 75, 100, 150 and 200 mV s⁻¹ and CO_{ad} stripping experiment of the catalysts were carried. For comparison, the curves of peak current density against the square root of scan rates of CVs were given in Fig. 3. The obtained linear relationship is attributed to a diffusion controlled process during the electrooxidation.³⁰ The relationship between the peak current and the square root of scan rates complies with the following equation where i_p is the peak current density, n is the electron-transfer number for the total reaction, n' is the electron transfer number in the rate-determining step, α is the electron transfer coefficient of the rate-determining step, A is the electrode surface area, C_∞ is the bulk concentration of the reactant, D_0 is the diffusion coefficient, ν is the potential scan rate:

$$i_p = 2.99 \times 10^5 n(\alpha n')^{1/2} A C_\infty D_0^{1/2} \nu^{1/2}$$

In the same electrolyte and the same reaction, the parameters n , C_∞ and D_0 are same. Thus, the slop of i_p vs. the square root of scan rates is determined by the term of $\alpha n'$. The corresponding slopes for Pt/C-C, Pt/C-H, PtCu/C-1, PtCu/C-2, PtCu/C-3, PtCu/C-4 and PtCu/C-5 are 24.3, 12.9, 24.3, 63.8, 42.1, 26.0 and 20.7, respectively. It shows that the electron transfer coefficients on these catalysts are in the order of PtCu/C-2 > PtCu/C-3 > PtCu/C-4 > Pt/C-C \approx PtCu/C-1 > PtCu/C-5 > Pt/C-H. This indicates that the fluffy nanoflower shape for PtCu/C-2, PtCu/C-3 and PtCu/C-4 greatly have advantages for the electron transfer during the methanol oxidation, leading to an improved catalytic

activity. From the CO_{ad} stripping curves (Fig. S5), it can be clearly seen that the peak potentials of CO_{ad} oxidation on all the PtCu/C catalysts shift to negative greatly compared with that of P/C-C and Pt/C-H. The negative shift indicated the promoted oxidative removal of CO_{ad} on the PtCu/C catalysts, which is consistent with the inference of XPS. In addition, with the help of citric acid, the electrochemical surface area (ECSA) for PtCu/C-3, PtCu/C-4, PtCu/C-5 is higher than PtCu/C-1 and PtCu/C-2 catalysts, calculated from the CO_{ad} stripping voltammetry results (Table S2), indicating the well-dispersed cluster structure benefits to the exposure of Pt sites. And the PtCu/C-3 with appropriate sized fluffy flower structure has slightly larger ECSA than PtCu/C-1 with burly nanospheric structure. The large ECSA combined with the electron transfer coefficient makes PtCu/C-3 the better catalytic activity for the oxidation of methanol than the other catalysts (Fig. 2).

Conclusions

We have developed a novel synthetic method to obtain dispersion-controlled PtCu/C catalysts by adjusting the concentration of citric acid during the galvanic replacement reaction of Cu to Pt. It was demonstrated that the dispersion have a great effect on the catalytic activity for methanol electrooxidation. Well-dispersed cluster structure benefits to the exposure of Pt sites, electron transfer and CO_{ad} oxidation. This work can be expected to open the door towards controlling the morphology of metal nanoclusters by addition of surfactant during the galvanic replacement reaction, consequently, resulting in tuning their physico-chemical characteristics.

This work was financially supported by the National Natural Science Foundation of China (No. 21373199), the National High Technology Research and Development Program of China (863 Program, Nos. 2012AA053401, 2013AA051002), the National Basic Research Program of China (973 Program, Nos. 2012CB932800, 2012CB215500 and 2011CB935702), the Strategic Priority Research Program of the Chinese Academy of Sciences (Grant No. XDA09030104) and the Science & Technology Research Programs of Jilin Province (Nos. 20102204, 20100420).

Notes and references

^a State Key Laboratory of Electroanalytical Chemistry, Changchun Institute of Applied Chemistry, Chinese Academy of Sciences, Changchun, Jilin, China. Fax: 86-431-85262225; Tel: 86-431-85262223; E-mail: xingwei@ciac.jl.cn

^b University of Chinese Academy of Sciences, Beijing, China

^c Laboratory of Advanced Power Sources, Changchun Institute of Applied Chemistry, 5625 Renmin Street, Changchun, Jilin, China; E-mail: liuchp@ciac.jl.cn

† Electronic Supplementary Information (ESI) available: See DOI: 10.1039/b000000x/

- Y. Qi, T. Bian, S.-I. Choi, Y. Jiang, C. Jin, M. S. Fu, H. Zhang and D. Yang, *Chemical Communications*, 2013.
- D.-M. Gu, Y.-Y. Chu, Z.-B. Wang, Z.-Z. Jiang, G.-P. Yin and Y. Liu, *Applied Catalysis B: Environmental*, 2011, **102**, 9-18.
- X. Z. Cui, J. L. Shi, L. X. Zhang, M. L. Ruan and J. H. Gao, *Carbon*, 2009, **47**, 186-194.
- L. Qian, L. Gu, L. Yang, H. Yuan and D. Xiao, *Nanoscale*, 2013.
- F. Ye, J. Yang, W. Hu, H. Liu, S. Liao, J. Zeng and J. Yang, *RSC Advances*, 2012, **2**, 7479-7486.
- H.-X. Liu, N. Tian, M. P. Brandon, Z.-Y. Zhou, J.-L. Lin, C. Hardacre, W.-F. Lin and S.-G. Sun, *ACS Catalysis*, 2012, **2**, 708-715.
- H. Yang, J. Zhang, K. Sun, S. Zou and J. Fang, *Angewandte Chemie International Edition*, 2010, **49**, 6848-6851.
- M. Yin, Y. Huang, L. Liang, J. Liao, C. Liu and W. Xing, *Chemical Communications*, 2011, **47**, 8172-8174.
- Y.-P. Xiao, S. Wan, X. Zhang, J.-S. Hu, Z.-D. Wei and L.-J. Wan, *Chemical Communications*, 2012, **48**, 10331-10333.
- Y. Tan, J. Fan, G. Chen, N. Zheng and Q. Xie, *Chemical Communications*, 2011, **47**, 11624-11626.
- J.-H. Jang, J. Kim, Y.-H. Lee, I. Y. Kim, M.-H. Park, C.-W. Yang, S.-J. Hwang and Y.-U. Kwon, *Energy & Environmental Science*, 2011, **4**, 4947-4953.
- C. Wang, M. F. Chi, D. G. Li, D. Strmcnik, D. van der Vliet, G. F. Wang, V. Komanicky, K. C. Chang, A. P. Paulikas, D. Tripkovic, J. Pearson, K. L. More, N. M. Markovic and V. R. Stamenkovic, *Journal of the American Chemical Society*, 2011, **133**, 14396-14403.
- Q. Li, P. Xu, B. Zhang, G. Wu, H. Zhao, E. Fu and H.-L. Wang, *Nanoscale*, 2013, **5**, 7397-7402.
- B. Y. Xia, H. B. Wu, X. Wang and X. W. Lou, *Journal of the American Chemical Society*, 2012, **134**, 13934-13937.
- R. Loukrakpam, P. Chang, J. Luo, B. Fang, D. Mott, I.-T. Bae, H. R. Naslund, M. H. Engelhard and C.-J. Zhong, *Chemical Communications*, 2010, **46**, 7184-7186.
- Q. Lv, M. Yin, X. Zhao, C. Li, C. Liu and W. Xing, *Journal of Power Sources*, 2012, **218**, 93-99.
- H. J. Qiu and F. X. Zou, *ACS Applied Materials & Interfaces*, 2012, **4**, 1404-1410.
- H.-H. Li, S. Zhao, M. Gong, C.-H. Cui, D. He, H.-W. Liang, L. Wu and S.-H. Yu, *Angewandte Chemie International Edition*, 2013, n/a-n/a.
- D. Xu, Z. Liu, H. Yang, Q. Liu, J. Zhang, J. Fang, S. Zou and K. Sun, *Angewandte Chemie International Edition*, 2009, **48**, 4217-4221.
- J. N. Tiwari, F.-M. Pan and K.-L. Lin, *New Journal of Chemistry*, 2009, **33**, 1482-1485.
- Y. Kang, L. Qi, M. Li, R. E. Diaz, D. Su, R. R. Adzic, E. Stach, J. Li and C. B. Murray, *ACS Nano*, 2012, **6**, 2818-2825.
- Y. Xu, Y. Yuan, A. Ma, X. Wu, Y. Liu and B. Zhang, *ChemPhysChem*, 2012, **13**, 2601-2609.
- Y. Xu, S. Hou, Y. Liu, Y. Zhang, H. Wang and B. Zhang, *Chemical Communications*, 2012, **48**, 2665-2667.
- Y. Xu and B. Zhang, *Chemical Society Reviews*, 2014, **43**, 2439-2450.
- B. Geboes, I. Mintsouli, B. Wouters, J. Georgieva, A. Kakaroglou, S. Sotiropoulos, E. Valova, S. Armanyanov, A. Hubin and T. Breugelmans, *Applied Catalysis B: Environmental*, 2014, **150-151**, 249-256.
- L. Chen, L. Kuai, X. Yu, W. Li and B. Geng, *Chemistry – A European Journal*, 2013, n/a-n/a.
- I. Mintsouli, J. Georgieva, E. Valova, S. Armanyanov, A. Kakaroglou, A. Hubin, O. Steenhaut, J. Dille, A. Papaderakis, G.

- Kokkinidis and S. Sotiropoulos, *J. Solid State Electrochem.*, 2013, **17**, 435-443.
- 28 H.-P. Liang, H.-M. Zhang, J.-S. Hu, Y.-G. Guo, L.-J. Wan and C.-L. Bai, *Angewandte Chemie International Edition*, 2004, **43**, 1540-1543.
- 5 29 I. Mintsouli, J. Georgieva, S. Armanyanov, E. Valova, G. Avdeev, A. Hubin, O. Steenhaut, J. Dille, D. Tsiplakides, S. Balomenou and S. Sotiropoulos, *Appl. Catal. B-Environ.*, 2013, **136**, 160-167.
- 10 30 . X. Z. Cui, J. L. Shi, L. X. Zhang, M. L. Ruan and J. H. Gao, *Carbon*, 2009, **47**, 186-194.
- 31 A. O. Neto, R. R. Dias, M. M. Tusi, M. Linardi and E. V. Spinace, *Journal of Power Sources*, 2007, **166**, 87-91.
- 32 X. Zhao, J. Zhu, L. Liang, J. Liao, C. Liu and W. Xing, *Journal of Materials Chemistry*, 2012, **22**, 19718-19725.
- 15 33. M. Yin, Y. Huang, Q. Li, J. O. Jensen, L. N. Cleemann, W. Zhang, N. J. Bjerrum and W. Xing, *ChemElectroChem*, 2014, **1**, 448-454.

20